Technology, 1969) (unpublished).

[18]V. Heine, Proc. Phys. Soc. (London) 81, 300 (1963).

[19]E. I. Blount, *Solid State Physics* (Academic, New York, 1962), Vol. 13, Appendix C.

[20]E. T. Copson, *Asymptotic Expansions* (Cambridge U. P., Cambridge, England, 1965).

[21]Hence, the error caused by this assumption can be estimated only after an E-k curve is computed and the actual energy distribution of tunneling electrons is available.

[22]ϕ_1 is taken to be less than ϕ_2.

[23]H. A. Antosiewicz and W. C. Rheinboldt, *Survey of Numerical Analysis* (McGraw-Hill, New York, 1962), Chap. 14, pp. 512–514.

[24]Numerical techniques used in this calculation are more fully discussed in Ref. 17.

[25]J. Franklin, J. Math. Anal. Applications 30, (1970).

[26]D. P. Foote and B. Kazan, Report No. ASO-TDR-63-640, 1963 (unpublished).

[27]P. Fielding, A. Fisher, and E. Mooser, J. Phys. Chem. Solids 8, 434 (1959); J. L. Brebner, *ibid.* 25, 1427 (1964); R. H. Bube and E. L. Lind, Phys. Rev. 115, 1159 (1959).

[28]T. C. McGill, S. Kurtin, and C. A. Mead, J. Appl. Phys. 41, 3831 (1970).

[29]The assistance of M. Simpson in the fabrication of this viewer is gratefully acknowledged.

[30]As a practical matter, a well-prepared substrate may contain several small regions of 5–15 structures each with nearly the same capacitance. Experience indicates that such a region contains, at its center, structures whose insulator thickness is uniform.

[31]This sort of inconsistency was noticed by Lewicki [G. W. Lewicki, Ph. D. thesis (California Institute of Technology, 1966) (unpublished); available from University microfilms, Ann Arbor, Michigan] in his study of AU-AlN-Al structures and attributed to wide tunneling distributions. The techniques discussed herein have been applied to Lewicki's data with notable success (see Ref. 17).

PHYSICAL REVIEW B VOLUME 3, NUMBER 10 15 MAY 1971

Mobility of Hot Electrons in n-Type InAs

R. C. Curby and D. K. Ferry
Department of Electrical Engineering, Texas Tech University, Lubbock, Texas 79409

(Received 26 October 1970)

A detailed study of the change in hot-electron mobility with applied electric fields in n-type InAs at 77 °K is presented. Both theoretical and experimental results are presented. Electron-electron collisions are assumed to be sufficiently frequent to determine the energy and momentum distribution of the electrons. The effects of ionized-impurity scattering are included in the momentum balance equation. The nonparabolicity of the conduction band is included in the theoretical calculation. The effect of the overlap integral which results in the nonparabolicity is included in the manner of Ehrenreich by utilizing several terms of the scattering matrix element. For low electric field (< 150 V/cm), a slight increase (approximately 10%) in the mobility with applied electric field is observed. For higher electric fields (> 150 V/cm), a strong decrease in the mobility with applied electric field occurs. This decrease is observed up to the point of impact ionization at approximately 800 V/cm.

INTRODUCTION

The mobility of hot electrons in polar semiconductors has become of interest in recent years with the production of III-V and II-VI compounds in relatively pure form. Most of the past work in III-V compounds has been for indium antimonide (InSb) and gallium arsenide (GaAs). For indium arsenide (InAs), some of the theories which have been applied to InSb can be used, since these materials have approximately the same band structure. In the present work, we calculate the transport properties for n-type InAs at 77 °K for applied electric fields below that required for the onset of impact ionization. There have been a few theories for InSb developed by using various approaches, and some of these may be, or have been, applied to InAs.

One of the earliest theories for InSb was presented by Ehrenreich.[1] He was one of the first to include the nonparabolicity of the energy band, doing so with the theory of Kane.[2] Kane's theory results from taking the interaction of the valence bands and the conduction band through the $\vec{k}\cdot\vec{p}$ terms of the Hamiltonian. The $\vec{k}$-independent spin-orbit interaction is also taken into account exactly. This refinement was necessary because the narrow band gap in these materials makes these interactions too strong for perturbation theory to yield accurate results. From these calculations, the relation between the energy bands $\mathcal{E}(\vec{k})$ and the crystal momentum $\hbar\vec{k}$ is no longer a simple parabolic relation, but is more nearly hyperbolic. Ehrenreich confined his calculation to temperatures above 200 °K to avoid problems arising from crystalline imperfections, such as ionized impurities.

The three major types of scattering for this temperature range were found to be polar optical-phonon scattering, electron-hole scattering, and acoustic-phonon scattering. The calculation included an extension of the transport theory first developed by Howarth and Sondheimer[3] to the case of nonparabolic conduction bands. This complex approach is necessitated by the failure of the relaxation-time approximation for polar optical-phonon scattering, which was found to be the dominant scattering mechanism over the temperature range 200–500 °K. Electron-hole scattering was present at all temperatures above 150 °K due to the intrinsic behavior of InSb in this range and became comparable to polar scattering at temperatures above 500 °K. This is a problem not encountered in InAs due to its larger band gap. Acoustic-phonon scattering was negligible for all temperature ranges considered.

Matz[4] presented calculations for InAs which are an extension of Ehrenreich's calculation, in that he included the case for high electric fields. He confined his calculation to temperatures greater than 200 °K, so that he considered only the effects of polar optical-phonon scattering. In addition, he included the change of the coupling constant for polar scattering due to the decrease of the overlap integral for the wave functions as the carrier energy is increased. The calculation yields a linear relation for the drift velocity versus applied electric field for electric fields below 1800 V/cm.

Another method, different from the theory given by Howarth and Sondheimer,[3] has been presented by Stratton.[5] He presented a calculation of the mobility of InSb for high electric fields, but below impact ionization, assuming that electron-electron collisions are sufficiently frequent to determine the energy and momentum distribution of the electrons. The electron distribution function in momentum space was assumed to be in internal equilibrium at a temperature T_e, which depends on the applied electric field, and was greater than the lattice temperature T_0. The temperature range assumed was high enough to consider the effects of polar optical scattering to be the only scattering mechanism present. In this diffusion approximation the collision operator for polar scattering is expanded in spherical harmonics, and the series is truncated after the first two terms. A drifted Maxwellian distribution function was assumed to approximate the distribution function. After averaging the collision operator over momentum and energy, the average rate of momentum loss and energy loss through collisions was equated to the average momentum and energy gain due to the electric field. From these balance equations, the drift velocity and mobility were calculated as a function of applied electric fields. For high temperatures, the calculation yields a slight increase in the mobility with applied electric fields (by a factor less than 2) and for low temperatures yields a large decrease (by a factor as great as 10) in the mobility with applied electric fields. The calculation is limited in that parabolic bands were assumed and only polar scattering was considered.

Dykman and Tomchuk[6] presented calculations which expanded Stratton's theory to the case of nonparabolic bands and included a calculation of the distribution function rather than assuming the Maxwellian distribution. However, the diffusion approximation was still used, so that only the first two terms f_0 and f_1 were calculated. It was observed that when the electron concentration was high enough, the exchange of energy between the electrons was more rapid than the exchange with the lattice, and the distribution function reduced to a Maxwellian even in relatively strong fields. The approach that Stratton[5] and Dykman and Tomchuk[6] present has the advantage over the approach presented by Ehrenreich[1] and Matz[4] in that there is a possibility of considering more than one type of scattering process at the same time.

Jones, Smith, and Beattie[7] presented a theoretical calculation of the drift velocity for InSb assuming a drifted Maxwellian distribution. The procedure used was to calculate the velocity as a function of energy in k space and then take an appropriate average using the drifted Maxwellian distribution. With this and the energy balance equation, they calculated the drift velocity as a function of applied electric field. One of the main drawbacks is that if there are competing scattering processes and one is involved primarily in momentum relaxation only and the other primarily in energy relaxation only, there is no way to take into account the one giving only momentum relaxation.

One of the newest methods for calculating drift velocity as a function of applied electric field for InAs and InSb was presented by Fawcett, Hilsum, and Rees.[8] They used a modified version of the Monte Carlo technique devised by Boardman, Fawcett, and Rees.[9] The band shape adopted for InAs was the nonparabolic one.[1] There is one major drawback to using this band structure for InAs in that it was approximated using the fact that the spin-orbit splitting of the valence bands of InSb was much larger than the band gap. This is not the case for InAs since the spin-orbit splitting is approximately equal to the energy gap, but Fawcett and Ruch[10] have shown that the error introduced is extremely small. Calculations of the drift velocity versus electric field show a linear relation between the two for applied electric fields below 1000 V/cm. These calculations were made for room temperature (300 °K), and they agree with Matz's calculation below 1000 V/cm. One of the problems

in using the Monte Carlo technique to calculate the distribution function and the drift velocity is that the calculation is essentially an empty-lattice approximation. Interactions with other electrons which lead to randomization of the momentum and energy are not considered. These effects which lead to energy diffusion, and consequently, a Maxwellian distribution function, are of considerable importance[11] and must be considered, especially in the case where the electron concentration is relatively high.

Along with these theoretical calculations, there have been various experimental results reported. Steele and Tosima[12] reported a linear relation for the drift velocity versus applied electric field for InAs at 300 °K. The low-field mobility of the material used was about 1.3×10^4 cm^2/V sec. This is rather low for InAs, which suggests that a large amount of compensating donors and acceptors was present in the crystal (N_d, $N_a = 10^{17}$ cm^{-3}), with consequent impurity scattering. Low-field Hall measurements showed the carrier concentration to be approximately 10^{15} cm^{-3}.

Bauer and Kuchar[13] reported a decrease in the mobility with an increase in applied electric field for electric fields between 250 V/cm and the onset of impact ionization at approximately 800 V/cm, but no detailed measurements were presented, since they were primarily interested in measuring ionization coefficients. This experiment was performed at 77 °K, which is lower than that of previous work. At this temperature, the effects of ionized-impurity scattering cannot be neglected as was done in the previous theoretical calculations. Experimental measurements have been presented by the present authors[14] and show a slight increase in mobility with applied electric fields for electric fields less than 200 V/cm, followed by the strong decrease observed previously. In fact, this mechanism is probably the dominant one at low electric fields for momentum relaxation.

It is the purpose of this report to present experimentally and theoretically a detailed study of the change in mobility versus applied electric field for n-type InAs at 77 °K, for electric fields below the onset of impact ionization. This temperature is below the range considered in previous theoretical work. Moreover, it is obvious that the additional effect of ionized-impurity scattering must be considered. Theoretical calculations of the mobility versus applied electric field are presented. The momentum and energy balance equations are used to calculate the drift velocity and electron temperature of the distribution in the diffusion approximation. One difference in the method used here from that presented by Stratton[5] is that the rate of energy and momentum loss for polar scattering is calculated directly rather than calculating the collision operator. The effects of ionized-impurity scattering are considered by adding the appropriate average rate of momentum loss to that of polar scattering. Also, the nonparabolicity of the energy bands is included. The decrease of the overlap integral is taken into account in the manner of Ehrenreich,[1] by utilizing several terms of the scattering matrix element.

HOT-ELECTRON TRANSPORT THEORY

Many of the transport properties of a pure semiconductor can be explained in terms of the band structure, which is the energy $\mathcal{E}(\vec{k})$ of an electron expressed as a function of its wave vector $\vec{k}$. The major feature of the band structure of the III-V compounds is known, but the detailed structure has not been established to the same degree as for germanium and silicon. The proposed band structure for InAs was calculated using Kane's theory with parameter values experimentally determined by Matossi and Stern.[15] Since the transport properties of the electrons are determined from the band structure of the conduction band, only the conduction-band structure will be considered. The band shape adopted for this is

$$\mathcal{E} - \mathcal{E}_c = \frac{\mathcal{E}_G}{2}\left[\left(1+\frac{2\hbar^2k^2}{m_c\mathcal{E}_G}\right)^{1/2} - 1\right], \tag{1}$$

where $\mathcal{E}_c$ is the minimum of the conduction band.

The momentum and energy balance equations are set up assuming that the momentum loss of the electrons is due to polar optical-phonon and ionized-impurity scattering, and that the energy loss of the electrons is due to polar optical-phonon scattering only. It can readily be shown that the losses to acoustic phonons are at least an order of magnitude smaller. Using these assumptions, the balance equations are given by

$$\left\langle\frac{d\mathcal{E}}{dt}\right\rangle_{\text{field}} + \left\langle\frac{d\mathcal{E}}{dt}\right\rangle_{\text{po}} = 0, \tag{2}$$

$$\left\langle\frac{dp}{dt}\right\rangle_{\text{field}} + \left\langle\frac{dp}{dt}\right\rangle_{\text{po}} + \left\langle\frac{dp}{dt}\right\rangle_{\text{imp}} = 0, \tag{3}$$

where the subscripts indicate the mechanism involved in the term. The subscript "field" indicates the change in the momentum and energy due to the applied electric force; "po" indicates the change due to polar optical phonons; and "imp" indicates the change due to ionized-impurity scattering.

The equations for the change in momentum and energy due to the applied electric field are quite simple and are given by

$$\left\langle\frac{d\mathcal{E}}{dt}\right\rangle_{\text{field}} = -ev_dE, \tag{4}$$

$$\left\langle\frac{dp}{dt}\right\rangle_{\text{field}} = -eE, \tag{5}$$

where $-e$ is the charge of an electron, E is the applied electric field, and v_d is the drift velocity of the electron. The average rate of momentum and energy loss for polar optical phonons and ionized-impurity scattering is not as easily obtained. To obtain these equations some of the basic quantities such as electron density and density of states must be recalculated to include the effects of the nonparabolic band structure.

Using the relation between $\vec{k}$ and $\mathcal{E}$ given in (1), the density of states becomes

$$N(\mathcal{E})\,d\mathcal{E} = \frac{1}{4\pi^2}\left(\frac{2m_c}{\hbar^2}\right)^{3/2}\left[\mathcal{E}\left(1+\frac{2\mathcal{E}}{\mathcal{E}_G}\right)\right]^{1/2}\left(1+\frac{2\mathcal{E}}{\mathcal{E}_G}\right), \tag{6}$$

where m_c is the effective mass at the band minimum at $\vec{k}=0$. It should be noted that the terms added which are not present for the parabolic case reduce to a value of 1 as $\mathcal{E}_G$ becomes $\gg\mathcal{E}$. A factor of 2 must still be added to (6) to account for spin degeneracy of the states.

To calculate the electron density, a distribution function must be assumed or known. For the materials with sufficiently high carrier concentration, the distribution function becomes a drifted Maxwellian,

$$f(\mathcal{E}) = a\,e^{-\mathcal{E}/k_0T_e}[1+(p_0p/m_c\,k_0T_e)], \tag{7}$$

where p_0 is the average momentum, for nonparabolic bands

$$\frac{m_cv_d}{(1-2m_cv_d^2/\mathcal{E}_G)^{1/2}},$$

in the direction of the applied electric field, and T_e is the equivalent electron temperature, both of which are parameters to be determined. The form of (7) for the distribution function is valid when electron-electron interactions dominate the randomization of the momentum. This is shown in the Appendix to be a valid assumption for the material used in the present experimental work for electron temperature T_e less than 287 °K. For simplicity $f(\mathcal{E})$ can be written as $f=f_0+f_1$, where $f_0=a\,e^{-\mathcal{E}/k_0T_e}$ and

$$f_1=(ap_0p/m_c\,k_0T_e)e^{-\mathcal{E}/k_0T_e}.$$

If the density of states from (6) and the distribution function from (7) are used, the electron density can be calculated from

$$n=\int_0^\infty N(\mathcal{E})f_0(\mathcal{E})\,d\mathcal{E}, \tag{8}$$

where it is assumed the energy is measured from $\mathcal{E}_c$ in (1). Equations (6) and (7) substituted into Eq. (8) yield

$$n=\int_0^\infty \frac{1}{2\pi^2}\left(\frac{2m_c}{\hbar^2}\right)^{3/2}\left[\mathcal{E}\left(1+\frac{\mathcal{E}}{\mathcal{E}_G}\right)\right]^{1/2}\times\left(1+\frac{2\mathcal{E}}{\mathcal{E}_G}\right)e^{-\mathcal{E}/k_0T_e}\,d\mathcal{E}. \tag{9}$$

Making the substitutions $\xi=\mathcal{E}/\mathcal{E}_G$ and $a=\mathcal{E}_G/k_0T_e$, Eq. (9) may readily be integrated to yield

$$n=\frac{1}{4\pi^2}\left(\frac{2m_c}{\hbar^2}\right)^{3/2}\frac{\mathcal{E}_G^{3/2}}{a}\,e^{a/2}K_2\left(\frac{a}{2}\right), \tag{10}$$

where $K_2(a/2)$ is the second-order modified Bessel function of the second kind.

Polar Optical-Phonon Scattering

Since our interest is in the high-mobility polar compounds, where the scattering process is comparatively weak, the calculation of the matrix element may be carried out for a weak-coupling coefficient between the carrier and the phonons. Thus, perturbation theory may be used to describe the interaction. The matrix element for this case was first derived by Frohlich[16] and Callen[17] and extended by Ehrenreich.[1] The matrix element obtained by using only s-symmetry wave functions may be written[1]

$$|(k\pm q|H_{po}|k)|^2=(2\pi\hbar^2eE_0/Vmq^2)(N_q+\tfrac{1}{2}+\tfrac{1}{2}\delta N_q), \tag{11}$$

where

$$eE_0=\frac{-m_ce^2\hbar\omega_0}{\hbar^2}\left(\frac{1}{\epsilon_0}-\frac{1}{\epsilon_\infty}\right); \tag{12}$$

ω_0 is the longitudinal optical-phonon frequency, ϵ_0 and ϵ_∞ are the dielectric constants for zero and infinite frequencies, respectively, and $\delta N_q=\pm1$ for phonon emission and absorption, respectively. Ehrenreich[1] presented a correction for the matrix element taking into account the admixture of the p-symmetry wave functions. This admixture of valence wave functions to the conduction-electron wave function arises due to the $\vec{k}\cdot\vec{p}$ interaction. It is precisely this admixture due to the conduction-band–valence-band interaction which leads to the presence of nonparabolicity in the conduction-band dispersion relation. The matrix element can, in general, be written in the form[1]

$$H_{k'k}=H_{k'k}^{(0)}+\eta H_{k'k}^{(1)}+\eta^2H_{k'k}^{(2)}, \tag{13}$$

where

$$\eta^2=\frac{\mathcal{E}}{\mathcal{E}_G(1+\mathcal{E}/\mathcal{E}_G)}. \tag{14}$$

Ehrenreich[1] points out that $H_{k'k}^{(i)}$ are generally all of the same magnitude with the exception that $H_{k'k}^{(1)}$ is 0 for polar scattering due to the symmetry. Then, to first order, the transition probability is

$$|H_{k'k}|^2=|H^{(0)}|^2+2\eta^2|H^{(2)}H^{(0)}|, \tag{15}$$

where $|H^{(0)}|^2$ is given by (11), and the second

term represents the correction terms for the nonparabolic bands. This correction term is effectively the result of the overlap integral. From the argument that the $H_{k'k}^{(i)}$ have the same magnitude, $|H^{(2)}H^{(0)}|$ can be replaced by the magnitude of $|H^{(0)}|^2$ without introducing much error. In practice, we use this approximation by letting $H^{(2)} = \lambda H^{(0)}$ and using λ as an adjustable parameter.

The probability per unit time of a carrier being scattered is

$$1/\tau = (2\pi/\hbar)\sum_{\vec{q}}[|(\vec{k}+\vec{q}, N_{\vec{q}}-1|H|\vec{k}, N_{\vec{q}})|^2 \times \delta(\mathcal{E}_{\vec{k}+\vec{q}, N_{\vec{q}}-1} - \mathcal{E}_{\vec{k}, N_{\vec{q}}}) + |(\vec{k}-\vec{q}, N_{\vec{q}}+1|H|\vec{k}, N_{\vec{q}})|^2 \times \delta(\mathcal{E}_{\vec{k}-\vec{q}, N_{\vec{q}}+1} - \mathcal{E}_{\vec{k}, N_{\vec{q}}})], \quad (16)$$

where the first term is the transition probability due to the absorption of a phonon and the second term is the transition probability due to the emission of a phonon. The summation over phonons shown in (16) may be converted to an integral over the variables q, ϕ, θ, with the k direction taken along the polar axis. The general approach is that given in Conwell, [18] and yields a solution of (16) as follows:

$$\frac{1}{\tau} = \frac{2eE_0}{(2m_c)^{1/2}\mathcal{E}^{1/2}(1+\mathcal{E}/\mathcal{E}_G)^{1/2}}\left[N_q\left(1+\frac{2(\mathcal{E}+\hbar\omega_0)}{\mathcal{E}_G}\right)\sinh^{-1}\left(\frac{\mathcal{E}(1+\mathcal{E}/\mathcal{E}_G)}{\hbar\omega_0(1+2\mathcal{E}/\mathcal{E}_G+\hbar\omega_0/\mathcal{E}_G)}\right)^{1/2}\right.$$
$$\left.+(N_q+1)\left(1+\frac{2(\mathcal{E}-\hbar\omega_0)}{\mathcal{E}_G}\right)\sinh^{-1}\left(\frac{\mathcal{E}(1+\mathcal{E}/\mathcal{E}_G)}{\hbar\omega_0(1+2\mathcal{E}/\mathcal{E}_G-\hbar\omega_0/\mathcal{E}_G)}-1\right)^{1/2}\right]. \quad (17)$$

Equation (17) gives only the contribution from the first term of the matrix element. Since the magnitude of the second term is two times the first term, $1/\tau_{po}$ can be written in the form

$$1/\tau_{po} = (1/\tau_{po})(1+2\eta^2), \quad (18)$$

where $1/\tau_{po}$ is the complete probability of scattering per unit time.

The rate of change of carrier energy due to polar optical scattering can be obtained from $\hbar\omega_0$ times the probability of a phonon being absorbed minus $\hbar\omega_0$ times the probability of a phonon being emitted. Using this fact, the rate of change of carrier energy can be found from (16). Carrying out the integration over q, as above, yields

$$\frac{d\mathcal{E}}{dt} = \frac{(1+2\eta^2)2eE_0\hbar\omega_0}{[2m_c\mathcal{E}(1+\mathcal{E}/\mathcal{E}_G)]^{1/2}}\left[N_q\left(1+\frac{2(\mathcal{E}+\hbar\omega_0)}{\mathcal{E}_G}\right)\sinh^{-1}\left(\frac{\mathcal{E}(1+\mathcal{E}/\mathcal{E}_G)}{\hbar\omega_0(1+2\mathcal{E}/\mathcal{E}_G+\hbar\omega_0/\mathcal{E}_G)}\right)^{1/2}\right.$$
$$\left.-(N_q+1)\left(1+\frac{2(\mathcal{E}-\hbar\omega_0)}{\mathcal{E}_G}\right)\sinh^{-1}\left(\frac{\mathcal{E}(1+\mathcal{E}/\mathcal{E}_G)}{\hbar\omega_0(1+2\mathcal{E}/\mathcal{E}_G-\hbar\omega_0/\mathcal{E}_G)}-1\right)^{1/2}\right]. \quad (19)$$

The average rate of energy loss per electron is found by taking an average over energy using a drifted Maxwellian distribution, as before. This average is defined by

$$\frac{d\mathcal{E}}{dt} = \int_0^\infty N(\mathcal{E})f_0(\mathcal{E})\frac{d\mathcal{E}}{dt}\,d\mathcal{E} \Big/ \int_0^\infty N(\mathcal{E})f_0(\mathcal{E})\,d\mathcal{E}. \quad (20)$$

Substituting (6) and (7) into (20) and changing the limit on the integration term for emission, (20) becomes

$$\frac{d\mathcal{E}}{dt} = A\int_0^\infty Q(\mathcal{E})\,e^{-\mathcal{E}/k_0T_e}\,d\mathcal{E} + \int_0^\infty Q(\mathcal{E})\frac{\mathcal{E}/\mathcal{E}_G}{1+2\mathcal{E}/\mathcal{E}_G}e^{-\mathcal{E}/k_0T_e}\,d\mathcal{E}, \quad (21)$$

where

$$A = \left(\frac{2}{m_c}\right)^{1/2}\frac{2eE_0\hbar\omega_0(e^{x_0-x_e}-1)}{\mathcal{E}_G^{1/2}k_0T_e\,e^{a/2}K_2(a/2)}N_q$$

and

$$Q(\mathcal{E}) = \left(1+\frac{2(\mathcal{E}+\hbar\omega_0)}{\mathcal{E}_G}\right)\left(1+\frac{2\mathcal{E}}{\mathcal{E}_G}\right)\times\sinh^{-1}\left(\frac{\mathcal{E}(1+\mathcal{E}/\mathcal{E}_G)}{\hbar\omega_0(1+2\mathcal{E}/\mathcal{E}_G+\hbar\omega_0/\mathcal{E}_G)}\right).$$

The various quantities are defined as follows: $x_0 = \hbar\omega_0/k_0T$; $x_e = \hbar\omega_0/k_0T_e$; $a = \mathcal{E}_G/k_0T_e$. The second integral is a result of the correction term on the matrix element. The argument of the inverse hyperbolic sine is simplified by making the assumption that the arcsinh is a slowly varying function of $\mathcal{E}$; therefore

$$\frac{\mathcal{E}(1+\mathcal{E}/\mathcal{E}_G)}{\hbar\omega_0(1+2\mathcal{E}/\mathcal{E}_G+\hbar\omega_0/\mathcal{E}_G)}$$

can be approximated by $\mathcal{E}/\hbar\omega_0$. Using this assumption and making the substitutions

$$\mathcal{E}/\hbar\omega_0=\sinh^2 q, \quad \hbar\omega_0/k_0T_e=x_e, \quad \mathcal{E}_G/k_0T_e=a,$$

(21) becomes

$$\left\langle\frac{d\mathcal{E}}{dt}\right\rangle=\hbar\omega_0 A\left[\int_0^\infty 2G_1(q)\,e^{-x_e\sinh^2 q}\,q\sinh q\cosh q\,dq + \int_0^\infty 2G_2(q)\,q\sinh q\cosh q\,dq\right],$$

where

$$G_1(q)=1+(4x_e/a)(\cosh^2 q+\sinh^2 q)+(4x_e^2/a^2)\cosh^2 q\sinh^2 q,$$

$$G_2(q)=(x_e/a)[\sinh^2 q+(2/a)\cosh^2 q\sinh^2 q].$$

The integration of this may readily be carried out and the result is

$$\left\langle\frac{d\mathcal{E}}{dt}\right\rangle=B[g_1(x_e)K_0(\tfrac{1}{2}x_e)+g_2(x_e)K_1(\tfrac{1}{2}x_e)], \tag{22}$$

where

$$B=\left(\frac{2T_e\theta_0}{m_c}\right)^{1/2}\frac{eE_0k_0N_q e^{x_e/2}(e^{x_0-x_e}-1)}{\mathcal{E}_G^{1/2}e^{a/2}K_2(a/2)}x_e^{1/2},$$

$$g_1(x_e)=2+\frac{4}{a}\left(1+\frac{2}{a}\right)-\frac{x_e}{2}+\frac{1}{2ax_e},$$

$$g_2(x_e)=\frac{2x_e}{a}\left(1+\frac{3}{a}\right)+\frac{x_e}{2}\left(1+\frac{3}{x_e a}\right),$$

and K_ν is the modified Bessel function of the second kind of order ν.

In order to complete the polar contribution to the balance equation, the rate of loss of crystal momentum by the carriers to the polar optical phonons is needed. This computation is simplified in that only the component of the momentum along the field direction need be calculated. Starting from perturbation theory, the rate of momentum change is given by

$$\frac{dp}{dt}=\frac{2\pi}{\hbar}\sum_q[\hbar q_E|(\vec{k}+\vec{q},N_{q-1}|H_{po}'|\vec{k},N_q)|^2\times\delta(\mathcal{E}_{\vec{k}+\vec{q},N_q-1}-\mathcal{E}_{\vec{k},N_q}) - \hbar q_E|(\vec{k}-\vec{q},N_q+1|H_{po}'|\vec{k},N_q)|^2\times\delta(\mathcal{E}_{\vec{k}-\vec{q},N_q+1}-\mathcal{E}_{\vec{k},N_q})]. \tag{23}$$

This is converted to an integral in the same manner as in (16). Integration is also carried out in the same manner with q_E given by

$$q_E=(k_E/k)q\cos\theta, \tag{24}$$

where k_E is the wave vector parallel to the electric field. The value used for $\cos\theta$ is that which makes the argument of the δ function in energy vanish and is

$$\cos\theta=\mp\frac{q}{k}+\frac{\hbar\omega_0 m_c}{\hbar^2 kq}\left(1+\frac{2\mathcal{E}}{\mathcal{E}_G}\pm\frac{\hbar\omega_0}{\mathcal{E}_G}\right), \tag{25}$$

where the upper sign is for phonon absorption and the lower sign is for phonon emission. Changing (23) to an integral and integrating, the momentum rate of loss is

$$\frac{dp}{dt}=(1+2\eta^2)eE_0\left(\frac{p_E}{p}\right)[F_1(\mathcal{E}+\hbar\omega_0)N_q+F_1(\mathcal{E}-\hbar\omega_0)(N_q+1)], \tag{26}$$

where

$$F_1(\mathcal{E}\pm\hbar\omega_0)=\left(1+\frac{2(\mathcal{E}\pm\hbar\omega_0)}{\mathcal{E}_G}\right)\left[\left(\frac{\mathcal{E}(1+\mathcal{E}/\mathcal{E}_G)\pm\hbar\omega_0(1+2\mathcal{E}/\mathcal{E}_G\pm\hbar\omega_0/\mathcal{E}_G)}{\mathcal{E}(1+\mathcal{E}/\mathcal{E}_G)}\right)^{1/2} - \frac{\hbar\omega_0}{\mathcal{E}(1+\mathcal{E}/\mathcal{E}_G)}\sinh^{-1}\left(\frac{\mathcal{E}(1+\mathcal{E}/\mathcal{E}_G)}{\hbar\omega_0(1+2\mathcal{E}/\mathcal{E}_G\pm\hbar\omega_0)}-\frac{1}{2}\pm\frac{1}{2}\right)^{1/2}\right].$$

The average rate of momentum loss per electron is found by taking an average over the energy using our drifted Maxwellian distribution. The spherically symmetric term $f_0(\mathcal{E})$ yields no contribution to the average momentum. The drift momentum arises from the $f_1(\mathcal{E})$ term in (7). The average rate of momentum loss is then

$$\frac{dp}{dt}=\frac{1}{n_0}\int_0^\infty N(\mathcal{E})f_1(\mathcal{E})\frac{dp}{dt}\,d\mathcal{E}. \tag{27}$$

Substituting the above equations into (27) and using the assumption already stated for arcsinh gives the results as

$$\left\langle\frac{dp}{dt}\right\rangle=A_P\left((e^{x_0-x_e}+1)\int_0^\infty F_2(\mathcal{E})e^{-\mathcal{E}/k_0T_e}\,d\mathcal{E} + (e^{x_0-x_e}-1)\int_0^\infty F_2(\mathcal{E})e^{-\mathcal{E}/k_0T_e}\,d\mathcal{E}\right), \tag{28}$$

where

$$A_P=\frac{4eEm_c v_d(1-2m_c v_d^2/\mathcal{E}_G)^{-1/2}}{3(2m_c)^{1/2}\mathcal{E}_G^{1/2}(k_0T_e)^2 e^{a/2}K_2(a/2)}N_q\,,$$

$$F_2(\mathcal{E})=\left[\left(1+\frac{2\mathcal{E}}{\mathcal{E}_G}\right)\left(1+\frac{2\mathcal{E}+\hbar\omega_0}{\mathcal{E}_G}\right)+\frac{\mathcal{E}}{\mathcal{E}_G}\left(1+\frac{\mathcal{E}+\hbar\omega_0}{\mathcal{E}_G}\right)\right]G_1(\mathcal{E}),$$

$$F_3(\mathcal{E})=\frac{F_2(\mathcal{E})}{G_1(\mathcal{E})}\left(1+\frac{2\mathcal{E}+\hbar\omega_0}{\mathcal{E}_G}\right)\sinh^{-1}\left(\frac{\mathcal{E}}{\hbar\omega_0}\right)^{1/2},$$

$$G_1(\mathcal{E})=\left[(\mathcal{E}+\hbar\omega_0)\mathcal{E}\left(1+\frac{\mathcal{E}}{\mathcal{E}_G}\right)\left(1+\frac{\mathcal{E}+\hbar\omega_0}{\mathcal{E}_G}\right)\right]^{1/2}.$$

Making the same substitutions

$$x_e=\hbar\omega_0/k_0T_e,\quad x_0=\hbar\omega_0/k_0T\,,$$

$$\mathcal{E}/\hbar\omega_0=\sinh^2 q,\qquad a=\mathcal{E}_G/k_0T_e,$$

Eq. (27) becomes

$$\left\langle\frac{dp}{dt}\right\rangle=A_P(\hbar\omega_0)^2\left((e^{x_0-x_e}+1)\int_0^\infty G_2(q)e^{-x_e\sinh^2 q}\,dq+2(e^{x_0-x_e}-1)\int_0^\infty G_3(q)e^{-x_e\sinh^2 q}\,q\sinh q\cosh q\,dq\right),\tag{29}$$

where

$$G_2(q)=2\left[1+\frac{4x_e}{a}\cosh 2q+\left(\frac{x_e}{a}\right)^2\sinh^2 2q\right]\times\left[1+\frac{2x_e}{a}\cosh 2q+\frac{1}{2}\left(\frac{x_e}{a}\right)^2\sinh^2 2q\right]^{1/2}\times\sinh^2 q\cosh^2 q+2\frac{x_e}{a}\left[\sinh^4 q\cosh^2 q+\frac{2x_e}{a}\sinh^4 q\cosh^4 q\right],$$

$$G_3(q)=1+\frac{4x_e}{a}\cosh 2q+\frac{x_e^2}{a}\sinh^2 2q+\frac{x_e}{a}\sinh^2 q\left(1+\frac{2}{a}\cosh^2 q\right).$$

The integration is straightforward and the rate of momentum loss is found to be

$$\frac{dp}{dt}=\frac{x_e}{2}A_P\exp\left(\frac{x_e}{2}\right)\left\{(e^{x_0-x_e}+1)\left[\frac{1-x_e+2/x_e a}{2a}K_0\left(\frac{x_e}{2}\right)+\left(1+\frac{x_e}{2a}+\frac{2}{x_e a^2}\right)K_1\left(\frac{x_e}{2}\right)+\frac{2x_e}{a}\left(1+\frac{1}{a}\right)K_2\left(\frac{x_e}{2}\right)\right]+(e^{x_0-x_e}+1)\left[\left(1+\frac{4}{a}+\frac{8}{a^2}\right)K_0\left(\frac{x_e}{2}\right)+\frac{2x_e}{a}\left(\frac{3}{a}+\frac{3}{4}\right)K_1\left(\frac{x_e}{2}\right)+\frac{x_e}{2a}\left(1+\frac{3}{a}\right)K_2\left(\frac{x_e}{2}\right)\right]\right\}.\tag{30}$$

Ionized-Impurity Scattering

We now turn our attention to ionized-impurity scattering, the dominant momentum relaxation process at low electric fields. Ionized-impurity scattering has a momentum relaxation time; therefore, the mobility can be written as

$$\mu=e\langle\tau\rangle/m_c\,.\tag{31}$$

In using the momentum and energy balance equations, the mobility is given by[18]

$$\mu=ev_d\Big/\left\langle\frac{dp}{dt}\right\rangle\,.\tag{32}$$

Equating (31) and (32), the average rate of momentum loss can be written as

$$\left\langle\frac{dp}{dt}\right\rangle=\frac{mv_d}{\langle\tau\rangle}\,.\tag{33}$$

The procedure for calculating the scattering time τ for nonparabolic bands is the same as for parabolic bands except for the calculation of the energy dependence of the velocity. The velocity is given by

$$v=(1/\hbar)\nabla_k\mathcal{E}(\vec{k}).\tag{34}$$

By using the energy relation from (1), (34) becomes

$$v=\left[\frac{2\mathcal{E}}{m_c}\left(1+\frac{\mathcal{E}}{\mathcal{E}_G}\right)^{1/2}\Big/\left(1+\frac{2\mathcal{E}}{\mathcal{E}_G}\right)\right].\tag{35}$$

In the Brooks-Herring formulation of the relaxation time for ionized-impurity scattering, τ is[19]

$$\frac{1}{\tau_{\rm imp}}=\frac{Z^2e^4N_I}{8\pi\epsilon^2m_c^2v^3}\ln\beta^2\,,\tag{36}$$

where

$$\beta^2=4me^2\epsilon k_0Tv^2/\hbar^2e^2N_I\,.\tag{37}$$

Using (35) in the last two equations gives

$$\frac{1}{\tau_{\rm imp}}=\frac{Z^2e^4N_I(1+2\mathcal{E}/\mathcal{E}_G)^3}{16\pi(2m_c)^{1/2}\epsilon^2\mathcal{E}^{3/2}(1+\mathcal{E}/\mathcal{E}_G)^{3/2}}\ln\beta^2\,,\tag{38}$$

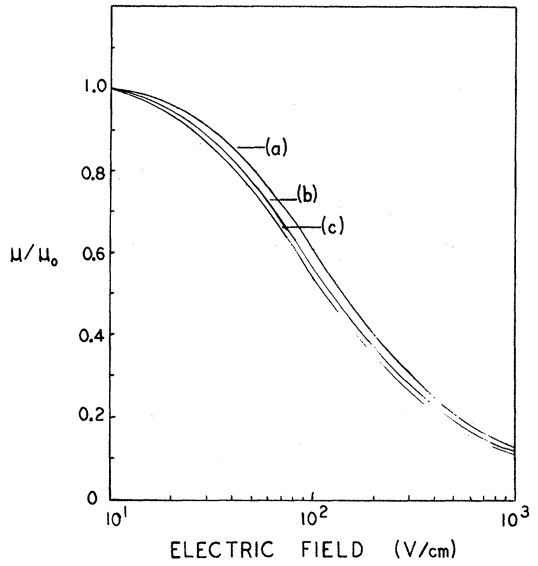

FIG. 1. Plot of normalized mobility versus applied electric field for polar optical-phonon scattering alone, for a fixed value of $\lambda = 3.5$ and (a) $E_0 = 2100$ V/cm, (b) $E_0 = 1800$ V/cm, and (c) $E_0 = 1700$ V/cm.

where now

$$\beta^2 = \frac{8m_c \epsilon k_0 T(1 + \mathcal{E}/\mathcal{E}_G)}{\hbar^2 e^2 N_I (1 + 2\mathcal{E}/\mathcal{E}_G)^2} . \tag{39}$$

The averaging function used for calculation, $\langle \tau \rangle$ is given by

$$\tau = \frac{m_c}{n_0} \int_0^\infty N(\mathcal{E}) \tau(\mathcal{E}) v_E^2 \frac{\partial f_0}{\partial \mathcal{E}} \, d\mathcal{E} . \tag{40}$$

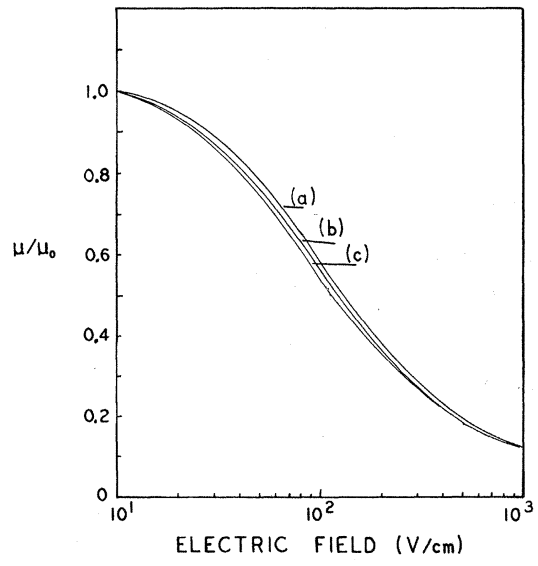

FIG. 2. Plot of normalized mobility versus applied electric field for polar optical-phonon scattering alone, for a fixed value of $E_0 = 1800$ V/cm and for (a) $\lambda = 6.5$, (b) $\lambda = 3.5$, and (c) $\lambda = 0$.

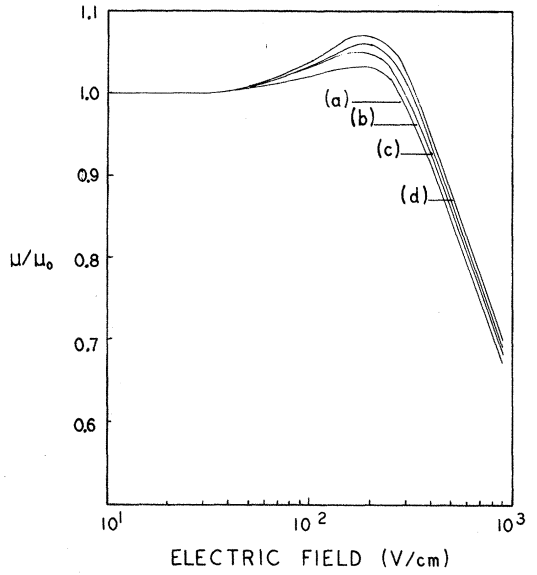

FIG. 3. Plot of normalized mobility versus applied electric field for ionized-impurity and polar optical-phonon scattering, for a fixed value of $\lambda = 3.5$ and for (a) $E_0 = 1700$ V/cm, (b) $E_0 = 1800$ V/cm, (c) $E_0 = 1900$ V/cm, and (d) $E_0 = 2100$ V/cm.

Assuming that the ln function is a slowly varying function of $\mathcal{E}$, it can be brought outside the integral and the energy-dependent terms replaced by their appropriate average. The resulting integral for (40) is

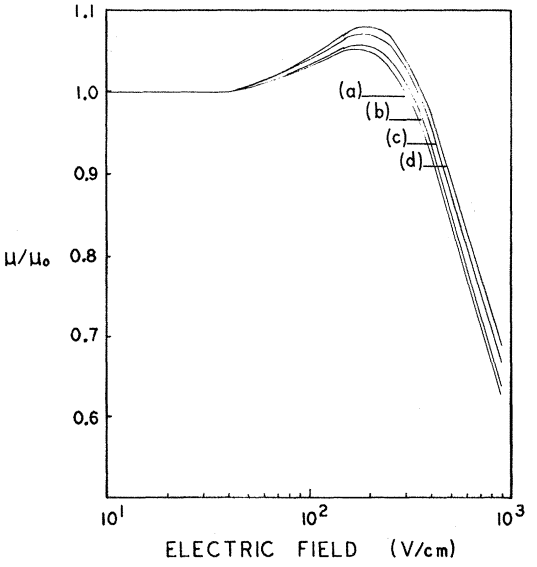

FIG. 4. Plot of normalized mobility versus applied electric field for ionized-impurity and polar optical-phonon scattering, for a fixed value of $E_0 = 1800$ V/cm and for (a) $\lambda = 5.0$, (b) $\lambda = 3.5$, (c) $\lambda = 2$, and (d) $\lambda = 0$.

$$\langle\tau\rangle = \frac{4}{3\theta\mathcal{E}_G^{1/2}(k_0T_e)^2 e^{a/2}K_2(a/2)} \times\int_0^\infty \frac{\mathcal{E}^3(1+\mathcal{E}/\mathcal{E}_G)^3}{(1+2\mathcal{E}/\mathcal{E}_G)^4} e^{-\mathcal{E}/k_0T_e}\, d\mathcal{E}\,, \quad (41)$$

where θ is $Z^2e^4N_I\ln(\beta^2)/16\pi(2m_c)^{1/2}\epsilon^2$. Carrying out the integrations, we have

$$\langle\tau\rangle = \frac{\pi^2(2m_c)^{1/2}\mathcal{E}_G^{7/2}}{e^4N_IZ^2 12(k_0T_e)^2K_2(a/2)} \times\left[\alpha_2\left(\frac{a}{2}\right) - \frac{3\exp(-a/2)}{a/2} + 3E_2\left(\frac{a}{2}\right) - E_4\left(\frac{a}{2}\right)\right](\ln\beta^2)^{-1}\,, \quad (42)$$

where α_i and E_i are exponential integrals and related to the incomplete γ functions as

$$E_n(z) = z^{n-1}\Gamma(1-n, z) \quad \text{and} \quad \alpha_n(z) = z^{-n-2}\Gamma(1-n, z).$$

The ionized impurities are fixed in the lattice and the collisions of the electrons with the ionized impurities are essentially elastic. Therefore, the change in the electron energy during the collision is negligible. The average rate of energy loss can then be taken to be

$$\left\langle\frac{d\mathcal{E}}{dt}\right\rangle_{\text{imp}} = 0. \quad (43)$$

For simplicity and ease of showing, first assume that polar optical-phonon scattering is the only scattering mechanism. Using Eqs. (22), (30), and (2)–(5), we get

$$mv_d^2 = (F^2/\mathcal{E}_G)[(1+\mathcal{E}_G^2/F)^{1/2} - 1]\,, \quad (44)$$

where

$$F = m_cv_d\left(1+\frac{2m_cv_d^2}{\mathcal{E}_G}\right)\left\langle\frac{d\mathcal{E}}{dt}\right\rangle\Big/\left\langle\frac{dp}{dt}\right\rangle\,. \quad (45)$$

Solving for the electric field, one obtains

$$E^2 = \left\langle\frac{d\mathcal{E}}{dt}\right\rangle\left\langle\frac{dp}{dt}\right\rangle\Big/v_de^2\left(1-\frac{2m_cv_d^2}{\mathcal{E}_G}\right)\,. \quad (46)$$

The mobility is defined as

$$\mu = v_d/E\,. \quad (47)$$

Figures 1 and 2 give a plot of μ/μ_0 versus applied electric field, where μ_0 is the low-field mobility and the lattice temperature is assumed to be 77 °K for various values of the coupling constant E_0 and the parameter λ. The low-field mobility μ_0 is 32×10^4 cm^2/V sec. There is almost an immediate falloff of the mobility with applied electric field.

With the aid of a computer the effects of ionized-impurity scattering can be included using the same procedure as for polar scattering alone. Figures 3 and 4 give a plot of μ/μ_0 versus applied electric field using the effects of both ionized-impurity scattering and polar optical-phonon scattering for an impurity concentration of 2×10^{16} cm^{-3}. The low-field mobility μ_0 is 6.10×10^4 cm^2/V sec. Figure 4 was computed using 1800 V/cm for the coupling constant E_0, which is lower than that calculated using (12). The reason for this is that the admixture of p-symmetry wave functions decreases the coupling between the electrons and polar optical phonons.[20] Figure 5 is a comparison between the present results and calculations assuming parabolic bands and calculations assuming nonparabolic band structure, but not including the correction in the matrix elements due to the admixture of the p-symmetry wave functions.

EXPERIMENTAL OBSERVATIONS

The samples used in obtaining data were cut from 1-mm slices of n-type InAs. The electron concentration was 2.0×10^{16} cm^{-3} and the electron mobility was 6×10^4 cm^2/V sec at 77 °K. The samples were cut from the slices into rectangular bars with the use of a wire saw. The cross section was approximately 0.8×0.8 mm^2. The cross section was first reduced by grinding the sample with a 600 grit slurry mix. After the sample cross section had been reduced to approximately 0.3×0.3 mm^2 in this manner they were chemically etched in the solution: 1 H_2O, 1 H_2O_2(30%), 1 H_2SO_4 (98%). The etchant removed any damaged surface caused by the wire saw and by the lapping process. The final samples had a cross-sectional area of approximately 0.25×0.25 mm^2. The sample lengths varied from 3.0 mm to 10.0 mm, and the sample impedance varied from 3 to 10 Ω, depending upon the length.

Electrical contacts were prepared by soldering a fine copper wire to the end of the sample using tin or indium metal. A wetting solution of 3 NH_3Cl (1 M), 27 $ZnCl_2$ (1 M), 100 H_2O was used to aid in soldering the contacts.

The samples were mounted in series with the center conductor of a 5.3-Ω strip line which was terminated with a 0.4-Ω resistor for monitoring the current through the sample. A coaxial delay-line–type pulse generator was constructed to supply the electric field needed. The pulse generator is a combination of a high-voltage dc power supply, eight coaxial cables connected in parallel (the length of which determines the pulse length), a coaxially mounted mercury-wetted relay, and a timing circuit for triggering the relay. The output impedance of the pulse generator was 6.5 Ω. The low impedance was accomplished by connecting eight 52-Ω coaxial cables in parallel. The rise time of the voltage pulse generator was ap-

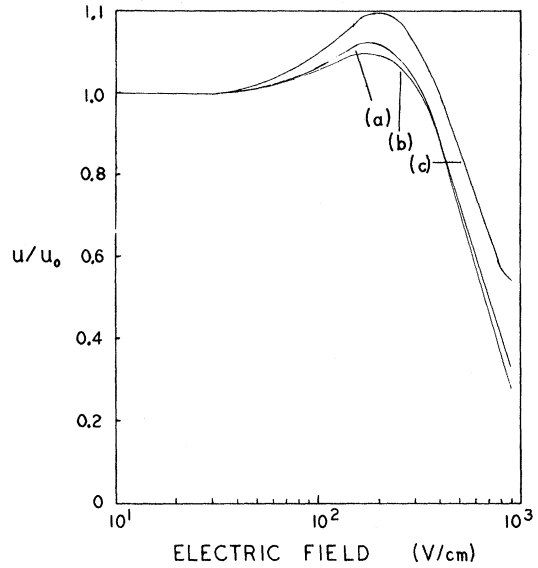

FIG. 5. Comparison of the three theories: (a) nonparabolic, $\lambda = 3.5$, $E_0 = 1800$ V/cm; (b) nonparabolic, $\lambda = 0$, calculated E_0; (c) parabolic, calculated E_0.

proximately 12 nsec.

The strip line with the sample mounted is immersed in a Dewar flask of liquid N_2 to reduce the sample's lattice temperature to 77 °K. A diagram of the complete experimental arrangement is shown in Fig. 6. For these short pulses (100 nsec), measurements of the voltage across the sample and current through the sample were taken using a 350 psec rise-time dual-trace sampling oscilloscope. The output of the sampling oscilloscope was connected to an x-y plotter to allow a permanent record of the I-V curve to be recorded. In Fig. 7, an I-V plot of a typical sample is shown.

In Fig. 8, a plot of μ/μ_0 versus applied electric field for two samples is shown. The third curve is for one of the samples with the voltage applied in the reverse direction to detect any effects due

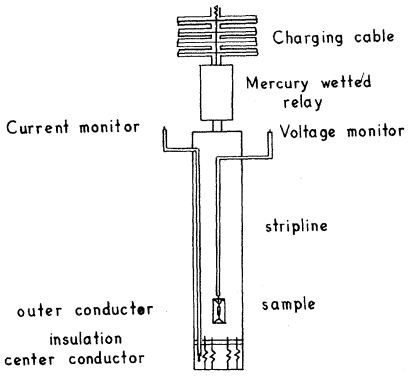

FIG. 6. Experimental arrangement.

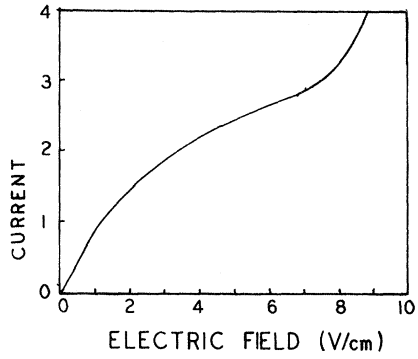

FIG. 7. I-E curve.

to contacts.

At low electric fields (< 150 V/cm) a slight increase in mobility is observed with increasing electric field. This increase is explained by the assumption that ionized-impurity scattering is the dominant momentum relaxation mechanism in this field range. For higher electric fields (> 150 V/cm) a strong decrease in the mobility with increasing electric field is observed. This decrease is due to polar optical phonons becoming the dominant momentum relaxation mechanism. As pointed out previously, polar optical-phonon scattering leads to a mobility an order of magnitude smaller than for acoustic-phonon scattering, so that the latter may be neglected.

Figure 8 also shows a comparison between experimental results and theoretical calculations. As in Fig. 3, the value of the coupling constant

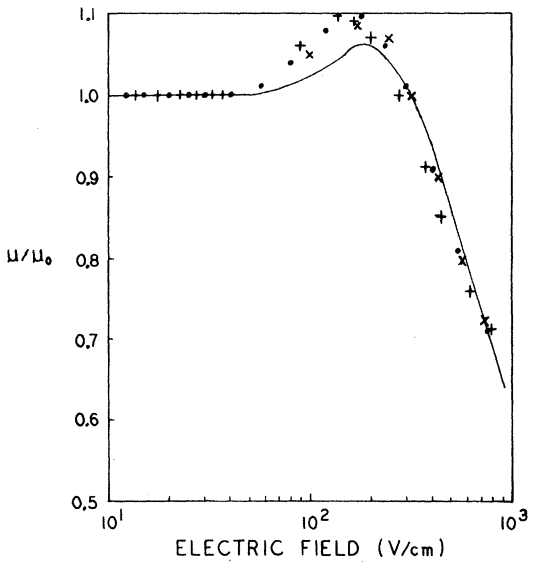

FIG. 8. Comparisons of theory and experiment: - theory; ○ sample $L1$; × sample L2; + sample L2, electric field reversed from first.

is 1800 V/cm and the magnitude of the correction term squared $H_{kk'}^{(2)}$ for a matrix element is 1.75 times $H_{kk'}^{(0)}$.

CONCLUSIONS

Figure 8 shows a comparison between experimental results and theoretical calculations. The agreement is very good for the low electric fields, below 100 V/cm. In the range where ionized-impurity scattering is still dominant, theoretical calculations of the mobility do not increase as rapidly as the experimental results indicate. This suggests that ionized-impurity scattering might increase faster than $T^{3/2}$ as is the case for a parabolic band structure.

At high electric fields (> 150 V/cm) polar optical-phonon scattering is dominant. Theoretical calculations of the mobility do not decrease as rapidly as the experimental results indicate. Several reasons for this are possible. First, the approximations made in solving the integrals for analytic solution would introduce some error. Second, the assumption of the matrix element derived for parabolic band structure instead of an exact matrix element, taking the effects of the nonparabolicity of the conduction band into account, would introduce the largest error into the calculations. Third, the assumption of a drifted Maxwellian distribution function allows more electrons at high energy than would be expected for the nonparabolic band structure, even with the electron-electron collisions randomizing the energy and momentum of the electrons.

APPENDIX A: CALCULATION OF CARRIER CONCENTRATION NEEDED FOR ASSUMPTION OF A MAXWELLIAN DISTRIBUTION

The rate of energy exchange between the electrons is given by Stratton as

$$\left(\frac{d\mathcal{E}}{dt}\right)_{e\text{-}e} \simeq \frac{ne^4}{4\pi\epsilon^2 p} \quad , \tag{A1}$$

where rationalized mks units are used. Carrying out the averaging integral, we obtain a function for the average rate of energy exchanged as[5]

$$\left\langle\frac{d\mathcal{E}}{dt}\right\rangle \simeq \left(\frac{1}{2m_c}\right)^{1/2} \frac{ne^4}{2\pi\epsilon^2} \frac{1+2k_0T_e/\mathcal{E}_G}{\mathcal{E}_G^{1/2}\, e^{\mathcal{E}_G/2k_0T_e} K_2(\mathcal{E}_G/2k_0T_e)} \, . \tag{A2}$$

The criterion for the distribution function to be Maxwellian is given by Stratton.[5] If the rate of energy exchange between electron-electron interactions is greater than or equal to the energy loss to the lattice due to electron polar optical-phonon interactions, then the distribution function is Maxwellian. This leads to the inequality

$$n \geq \frac{2\pi\epsilon^2}{e^4} \left\langle\frac{d\mathcal{E}}{dt}\right\rangle_{po} \frac{\mathcal{E}_G^{1/2}\, e^{\mathcal{E}_G/2k_0T_e} K_2(\mathcal{E}_G/2k_0T_e)(2m_c)^{1/2}}{1+2k_0T_e/\mathcal{E}_G} \, , \tag{A3}$$

where $\langle d\mathcal{E}/dt\rangle_{po}$ is defined in (22). For the material used in the experimental work (A3) yields the result that the distribution function is Maxwellian for electron temperatures below 300 °K.

[1] H. Ehrenreich, Phys. Chem. Solids 2, 131 (1957).

[2] E. D. Kane, Phys. Chem. Solids 1, 249 (1957).

[3] D. J. Howarth and E. H. Sondheimer, Proc. Roy. Soc. (London) A219, 53 (1953).

[4] O. Matz, Phys. Rev. 168, 843 (1967).

[5] R. Stratton, Proc. Roy. Soc. (London) A246, 406 (1958).

[6] I. M. Dykman and P. M. Tomchuk, Fiz. Tverd. Tela 8, 1343 (1966) [Sov. Phys. Solid State 8, 1075 (1966)].

[7] G. Jones, G. Smith, and A. R. Beattie, Phys. Status Solidi 20, K135 (1967).

[8] W. Fawcett, C. Hilsum, and H. D. Rees, Solid State Commun. 7, 1257 (1969).

[9] A. Boardman, W. Fawcett, and H. D. Rees, Solid State Commun. 6, 305 (1968).

[10] W. Fawcett and J. Ruch (unpublished).

[11] See, e.g., I. B. Levinson, Fiz. Tverd Tela 6, 2113 (1964) [Sov. Phys. Solid State 6, 1665 (1965)]; W. P. Dumke, Phys. Rev. 167, 783 (1968).

[12] M. C. Steele and S. Tosima, Japan. J. Appl. Phys. 2, 381 (1963).

[13] G. Bauer and F. Kuchar, Phys. Letters 30A, 399 (1969).

[14] R. C. Curby and D. K. Ferry, Phys. Letters 32A, 237 (1970).

[15] O. Madelung, *Physics of III-V Compounds* (Wiley, New York, 1964), p. 69.

[16] H. Frohlich, Proc. Roy. Soc. (London) A160, 230 (1937).

[17] H. Callen, Phys. Rev. 87, 1394 (1949).

[18] E. M. Conwell, *High Field Transport in Semiconductors* (Academic, New York, 1967), pp. 155–160.

[19] R. A. Smith, *Semiconductors* (Cambridge U. P., Cambridge, England, 1964), p. 150.

[20] H. Ehrenreich, Phys. Chem. Solids 9, 129 (1959).